Electronic Supplementary Material (ESI) for Journal of Materials Chemistry C.

Nickel Cobaltite/Multi-walled Carbon Nanotube Flexible Sensor for the Electrochemical Detection of Dopamine Released by Human Neural Cells

Rasha Rahman Poolakkandy[†], Neelakandan Annamalai Ramalakshmi[δ], Muhammed Fasil Puthiyaparambath[‡], Rajanikant Golgodu Krishnamurthy[δ], Raghu Chatanathodi[‡], and Mini Mol Menamparambath[†,]*

[†] Department of Chemistry, National Institute of Technology Calicut, Calicut-673601, Kerala, India

δ School of Biotechnology, National Institute of Technology Calicut, Calicut-673601, Kerala, India

‡ Department of Physics, National Institute of Technology Calicut, Calicut-673601, Kerala, India

Chemicals and reagents

Nickel (II) chloride (Alfa Aesar, B22085, 98%), cobalt (II) chloride (Fisher Scientific, 22643, 97%), urea (Fisher Scientific, 20885, 99%), n-butanol (Fisher Scientific, 71-36-3), multiwalled carbon nanotube (4-6 nm diameter and 5-20 µm length, TMC 220-05), Hydroxypropyl methyl cellulose (Himedia, 9004-65-3), dopamine hydrochloride (Sigma-Aldrich, 62-31-7, 98%), L-ascorbic acid (Sigma-Aldrich, 50-81-7, 99%), uric acid (Alfa Aesar, A13346, 99%), nafion D-520 dispersion (Alfa Aesar, 42118), L-Dopa (Sigma-Aldrich, D9628), ethanol (Changshu Hongsheng Fine Chemical Co. Ltd., Analytical reagent grade), polyimide heat resistant adhesive tape (Kapton 50mm), copper foil tape (Electomania), pyrolytic graphite sheet (Intelligent materials Pvt. Ltd., 7440-44-0), conductive silver paste (Techinstro, Silverpaste-001) were used as procured. SH-SY5Y cells were procured from National Centre for Cell

Science, Pune) and were maintained in DMEM/F12 (Thermo Fisher Scientific, MA, USA) containing 10% fetal bovine serum (FBS; Thermo Fisher Scientific, MA, USA) and 1% penicillin-streptomycin (Thermo Fisher Scientific, MA, USA). All chemicals required for artificial sweat preparation was procured from Sigma-Aldrich. Deionized (DI) water (> 18 MΩ) was used all through the synthesis. 0.1 molar phosphate buffer solution of pH 7.2 was used for the electrochemical studies.

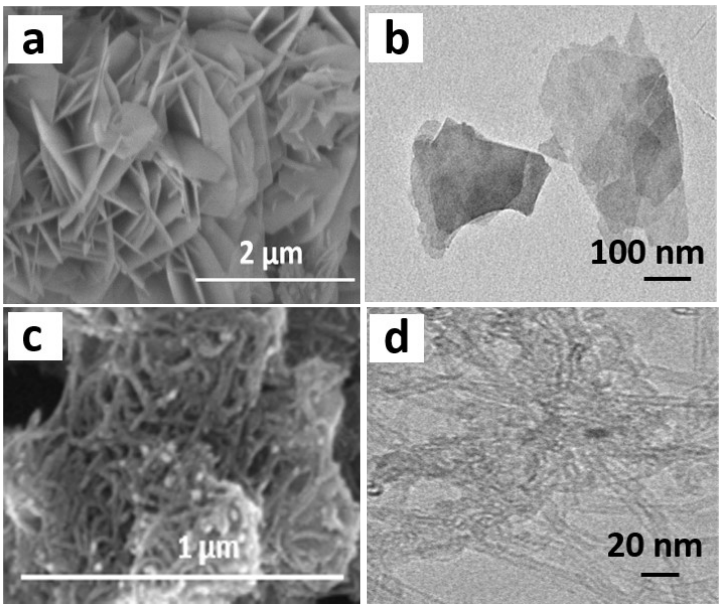

Supporting figure S1. (a) FESEM and (b) HRTEM of individual NC nanoflakes and (c) FESEM and (d) HRTEM of MWCNT dispersed using HPMC solution.

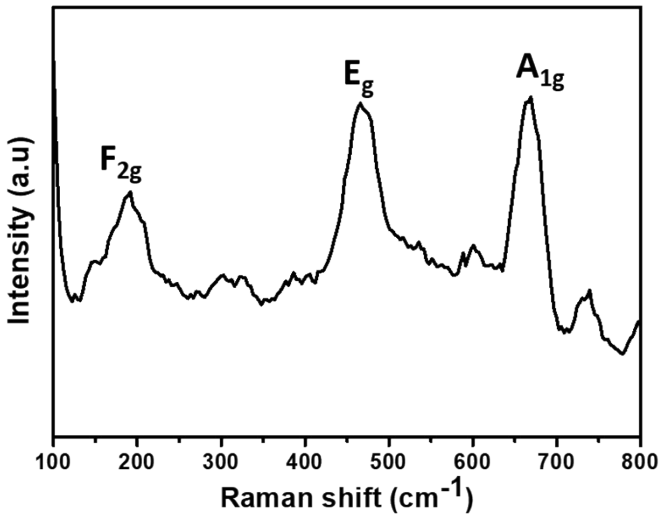

Supporting figure S2. Raman spectra of NC. The major peaks obtained at 187, 472 and 670 cm^{-1} corresponds to the F_{2g}, E_g and A_{1g} modes of NC.[1,2]

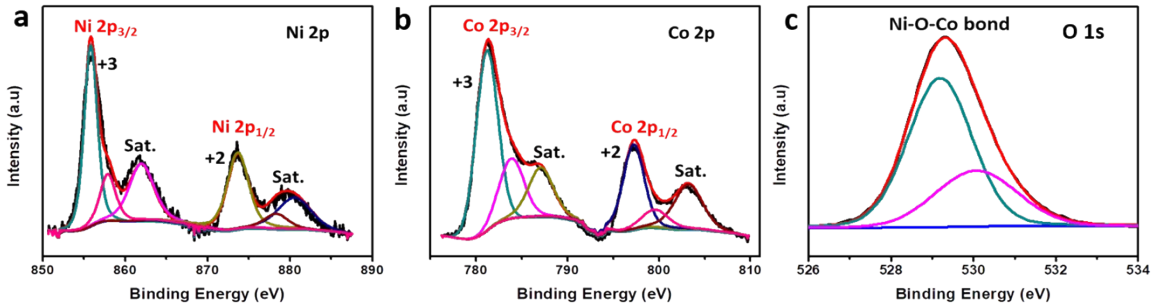

Supporting figure S3. Deconvoluted XPS spectra of (a) Ni (b) Co and (c) O of NC

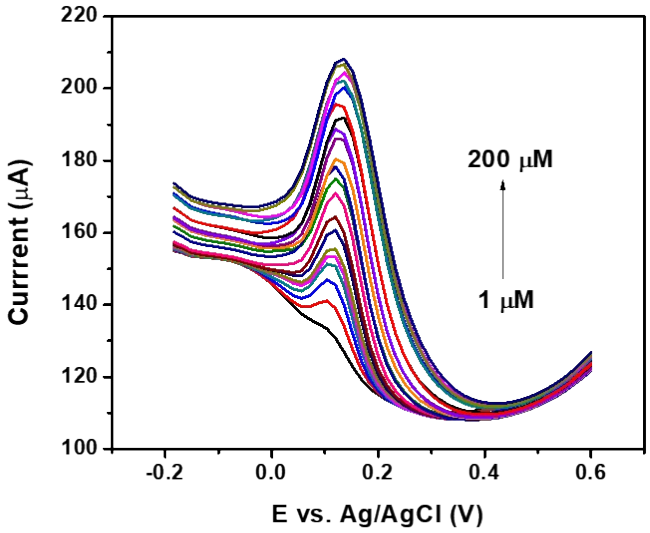

Supporting figure S4. DPV plots of NC/MWCNT modified GCE towards varying concentrations of DA.

Sl No.	Electrode	Linear range (μM)	LOD (μM)	Real Sample	Reference
1	CAuNE	1 – 100	5.83	Neural cells	S3
2	CuTRZMoO$_4$@ppy-2	1 – 100	0.080	Serum	S4
3	Au-SiO$_2$/GCE	1 – 100 100 – 500	1.98	Serum	S5
4	OM-ZnFe$_2$O$_4$-40	0.002 – 0.6	0.0004	PC12 cells	S6
5	DAP-ERGO/MoO3	0.1 – 900	0.025	Urine	S7
6	Pt-Ni/rGO	0.01 – 100	0.0026	Serum, pharmaceuti cal drug	S8

7	Pd-NP/RGO	1 - 150	0.233	Injection	S9
8	ZnO NSB/GF	1 - 180	0.01	Urine	S10
9	SPCE/CQD	1 - 7	0.099	Urine	S11
10	NC/MWCNT	1 - 200	0.080	Neural cells, artificial sweat, serum	This work

Supporting table S1. Comparison of linear range, LOD and the real sample analysis of the proposed sensor with the literature.

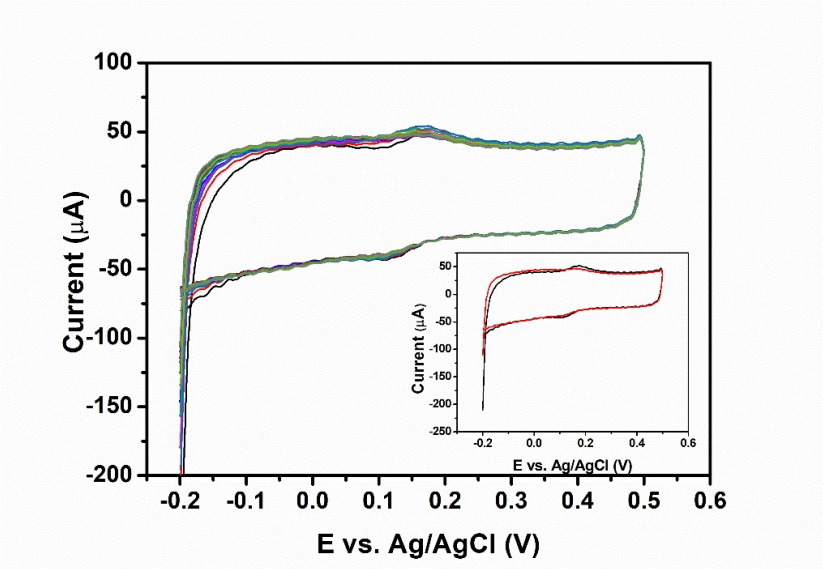

Supporting figure S5. Successive CV plots of NC/MWCNT modified electrodes in 100 μM DA solution. Inset showing the CV plot for the first and 20th cycle. The anodic peak current of first cycle is 51.9 μA and the anodic peak current after 20 cycles is 47.7 μA.

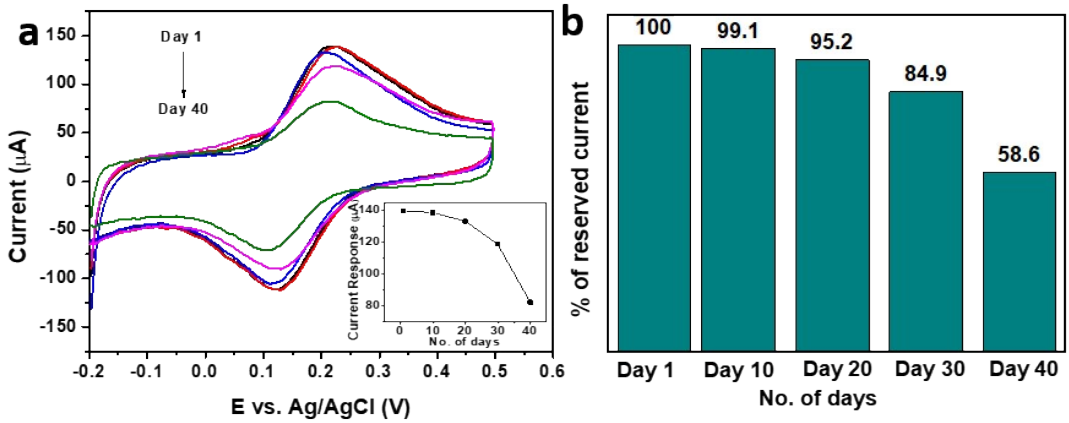

Supporting figure S6. Storage stability studies of NC/MWCNT modified electrode. (a) CV plots of NC/MWCNT modified electrode towards 1 mM DA taken periodically from day 1 to day 40. The inset showing the depletion in the anodic current with the number of days. (b) % of current reserved from day 1 to 40.

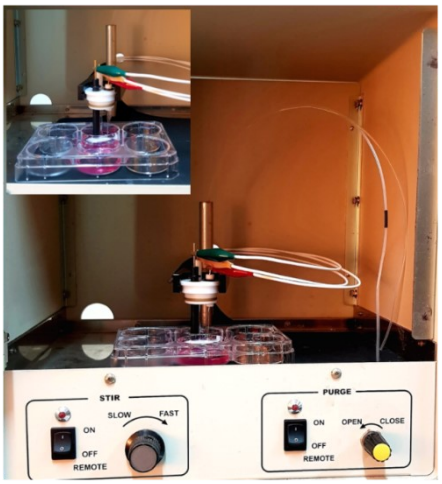

Supporting figure S7. Photograph of the amperometric detection setup for the detection of DA released by SH-SY5Y neural cells.

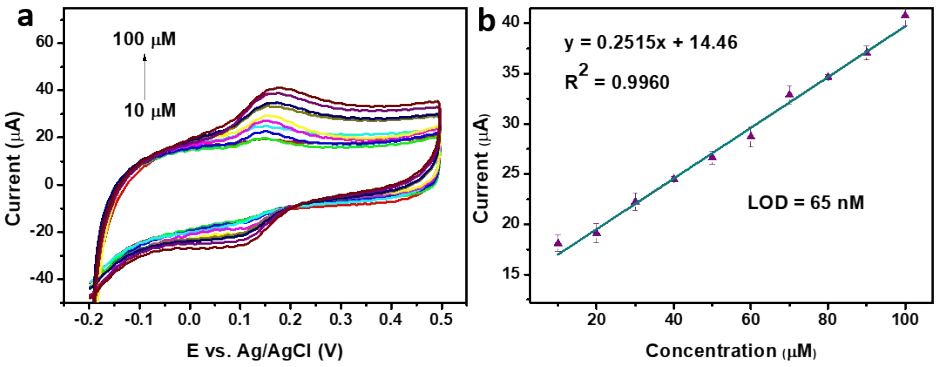

Supporting figure S8. (a) CV plots of NC/MWCNT modified GCE at different concentrations of DA from 10-100 µM in artificial sweat sample (b) The calibration plot of current response vs. concentration of DA.

Sl No.	Added	Output	Output	Recovery	%	RSD

	concentration (µM)	current in std. solution (µA)	current in sweat solution (µA)	concentration (µM)	Recovery	(%)
1	10	16.1	18.78	13.27	132.7	0.82
2	20	18.9	19.11	22.5	112.5	0.95
3	30	21.15	22.23	32.86	109.53	0.86
4	40	23.43	24.51	40.51	101.27	0.22
5	50	25.46	26.63	49.31	98.62	0.67
6	60	28.2	28.71	58.06	96.76	0.96
7	70	31.2	32.89	70.80	101.14	0.91
8	80	33.67	34.65	78.25	97.81	0.25
9	90	36.3	37.07	87.95	97.72	0.72
10	100	39.1	40.78	100.5	100.5	0.98

Supporting table S2. Recovery results of DA in artificial sweat

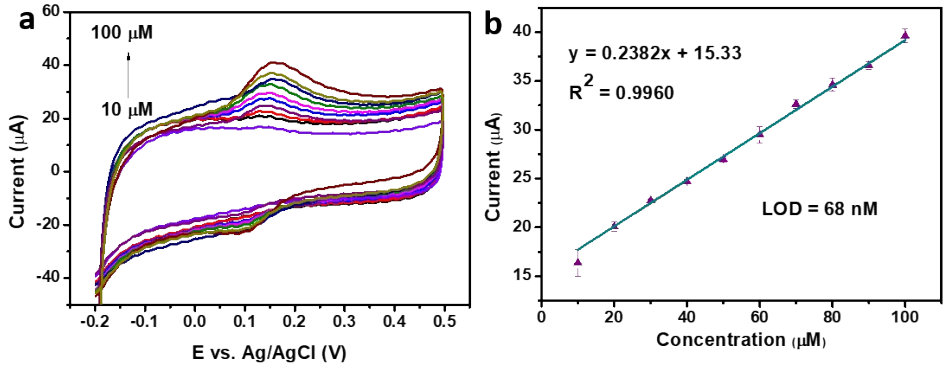

Supporting figure S9. (a) CV plots of NC/MWCNT modified GCE at different concentrations of DA from 10-100 µM in human serum sample (b) The calibration plot of current response vs. concentration of DA.

Sl No.	Added concentration (µM)	Output current in std. solution (µA)	Output current in sweat solution (µA)	Recovery concentration (µM)	% Recovery	RSD (%)
1	10	16.1	16.34	11.27	112.7	0.82
2	20	18.9	20.06	22.5	112.5	0.95
3	30	21.15	22.74	32.86	109.53	0.86
4	40	23.43	24.71	40.51	101.27	0.22
5	50	25.46	26.67	49.31	98.62	0.67
6	60	28.2	29.49	58.06	96.76	0.96
7	70	31.2	32.62	70.80	101.14	0.91
8	80	33.67	34.61	78.25	97.81	0.25

9	90	36.3	36.56	87.95	97.72	0.72
10	100	39.1	40.54	100.5	100.5	0.98

Supporting table S3. Recovery results of DA in human serum sample

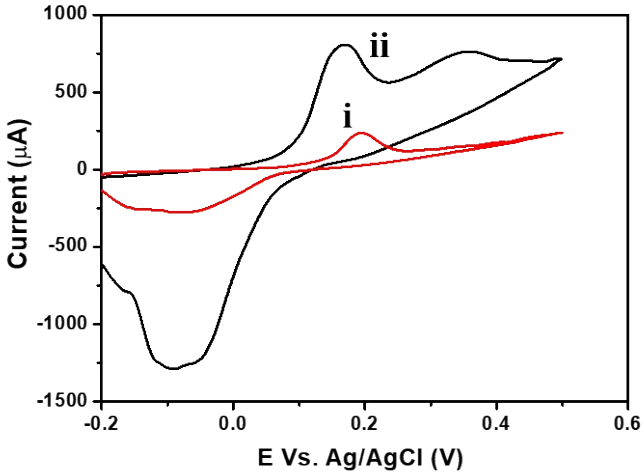

Supporting figure S10. CV response of the all-integrated sensor towards the (i) buffer solution and (ii) 100 nM DA.

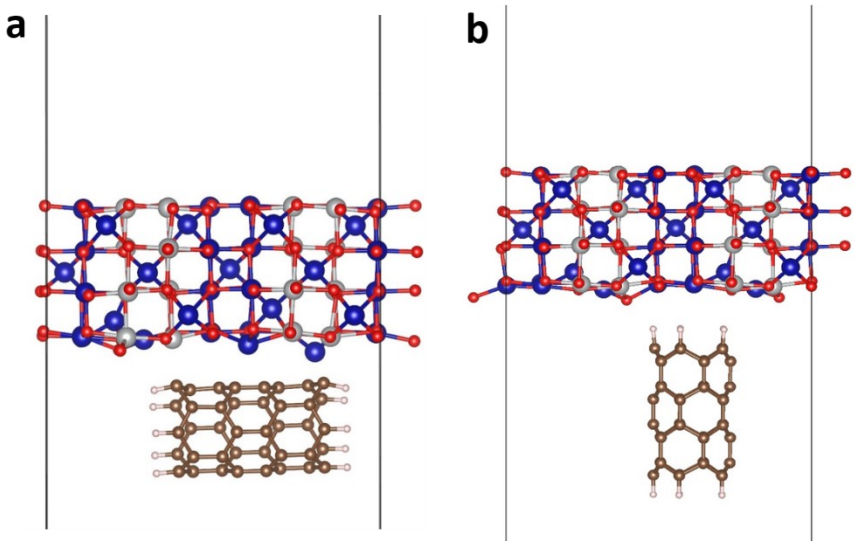

Supporting figure S11. The two initial configurations for the co-adsorption of passivated MWCNT below NC sheets.

References

1 D. Zhang, H. Yan, Y. Lu, K. Qiu, C. Wang, C. Tang, Y. Zhang, C. Cheng and Y. Luo, *Nanoscale Res. Lett.*, 2014, **9**, 1–9.

2 K. J. Kim and T. Y. Koh, *J. Sol-Gel Sci. Technol.*, 2016, **77**, 528–533.

3 D. S. Kim, E. S. Kang, S. Baek, S. S. Choo, Y. H. Chung, D. Lee, J. Min and T. H. Kim, *Sci. Rep.*, 2018, **8**, 1–10.

4 K. Zhou, D. Shen, X. Li, Y. Chen, L. Hou, Y. Zhang and J. Sha, *Talanta*, 2020, **209**, 120507.

5 S. Immanuel, T. K. Aparna and R. Sivasubramanian, *Surfaces and Interfaces*, 2019, **14**, 82–91.

6 Y. Huang, Y. Tang, S. Xu, M. Feng, Y. Yu, W. Yang and H. Li, *Anal. Chim. Acta*, 2020, **1096**, 26–33.

7 N. Roy, S. Yasmin and S. Jeon, *Microchem. J.*, 2020, **153**, 104501.

8 Y. Veera Manohara Reddy, B. Sravani, H. Maseed, T. Łuczak, M. Osińska, L. Subramanyamsarma, V. V. S. S. Srikanth and G. Madhavi, *New J. Chem.*, 2018, **42**, 16891–16901.

9 S. Palanisamy, S. Ku and S. M. Chen, *Microchim. Acta*, 2013, **180**, 1037–1042.

10 S. Huang, S. Song, H. Yue, X. Gao, B. Wang and E. Guo, *Sensors Actuators, B Chem.*, 2018, **277**, 381–387.

11 N. R. Devi, T. H. V. Kumar and A. K. Sundramoorthy, *J. Electrochem. Soc.*, 2018, **165**, G3112–G3119.